22. Artini, M. *et al.* Elevated serum levels of 90K/MAC-2 BP predict unresponsiveness to alpha-interferon therapy in chronic HCV hepatitis patients. *J. Hepatol.* **25**, 212–217 (1996).
23. Cheung, K. J. *et al.* The HCV serum proteome: a search for fibrosis protein markers. *J. Viral. Hepat.* **16**, 418–429 (2009).
24. Kuno, A. *et al.* Focused differential glycan analysis with the platform antibody-assisted lectin profiling for glycan-related biomarker verification. *Mol. Cell. Proteomics* **8**, 99–108 (2008).
25. Kuno, A. *et al.* Evanescent-field fluorescence-assisted lectin microarray: a new strategy for glycan profiling. *Nat. Met.* **2**, 851–856 (2005).
26. Vallet-Pichard, A. *et al.* FIB-4: an inexpensive and accurate marker of fibrosis in HCV infection. Comparison with liver biopsy and fibrotest. *Hepatology* **46**, 32–36 (2007).
27. Ito, K. *et al.* LecT-Hepa, a glyco-marker derived from multiple lectins, as a predictor of liver fibrosis in chronic hepatitis C patients. *Hepatology* **56**, 1448–1456 (2012).
28. Bruno, S. *et al.* Sustained virological response to interferon-α is associated with improved outcome in HCV-related cirrhosis: A retrospective study. *Hepatology* **45**, 579–587 (2007).
29. Cardoso, A.-C. *et al.* Impact of peginterferon and ribavirin therapy on hepatocellular carcinoma: Incidence and survival in hepatitis C patients with advanced fibrosis. *J. Hepatol.* **52**, 652–657 (2010).
30. Morgan, T. R. *et al.* Outcome of sustained virological responders with histologically advanced chronic hepatitis C. *Hepatology* **52**, 833–844 (2010).
31. Lupberger, J. *et al.* EGFR and EphA2 are host factors for hepatitis C virus entry and possible targets for antiviral therapy. *Nat. Med.* **17**, 589–595 (2011).
32. Iwasaki, Y. *et al.* Risk factors for hepatocellular carcinoma in hepatitis C patients with sustained virologic response to interferon therapy. *Liver Int.* **24**, 603–610 (2004).
33. Ikeda, K. *et al.* Anticarcinogenic impact of interferon on patients with chronic hepatitis C: A large-scale long-term study in a single center. *Intervirology* **49**, 82–90 (2006).
34. Kurosaki, M. *et al.* Data mining model using simple and readily available factors could identify patients at high risk for hepatocellular carcinoma in chronic hepatitis C. *J. Hepatol.* **56**, 602–608 (2012).
35. Schuppan, D. & Pinzani, M. Anti-fibrotic therapy: lost in translation? *J. Hepatolol.* **56**, S66–74 (2012).
36. Rizzo, L. *et al.* Comparison of transient elastography and acoustic radiation force impulse for non-invasive staging of liver fibrosis in patients with chronic hepatitis C. *Am. J. Gastroenterol.* **106**, 2112-2120 (2011).
37. Ferraioli, G. *et al.* Performance of real-time sitrain elastography, transient elastgraphy, and aspartate-to-platelet ration index in the assessment of fibrosis in chronic hepatitis C. *AJR Am. J. Roentgenol.* **199**, 19–25 (2012).
38. Poynard, T. *et al.* Standardization of ROC curve areas for diagnostic evaluation of liver fibrosis markers based on prevalences of fibrosis stages. *Clin. Chem.* **53**, 1615–1622 (2007).
39. Nishimura, S. Toward automated glycan analysis. *Adv. Carbohydr. Chem. Biochem.* **65**, 219–271 (2011).

Acknowledgments

This work was supported in part by a grant from New Energy and Industrial Technology Development Organization of Japan. We thank H. Ozaki, H. Shimazaki, S. Unno, K. Saito, M. Sogabe, Y. Kubo, J. Murakami, S. Shirakawa, T. Fukuda (AIST), and H. Naganuma (NCU) for technical assistance. We also thank A. Togayachi, T. Sato, H. Kaji, J. Hirabayashi, H. Tateno, A. Takahashi (AIST) and C. Tsuruno, S. Nagai and Y. Takahama (Sysmex Co.) for critical discussion.

Author contributions:

A.K. conceived and designed the study, performed most of the biochemical experiments, analyzed data and wrote the paper with comments from Y.T., M.M. and H.N.; Y.I. conceived and designed the study, performed the sample pre-treatment for the assay, and analyzed data; Y.T., K.I., M.M., and S.H collected clinical samples, designed the validation study, and analyzed data; A.M. and S.S. performed the biochemical experiments including lectin microarray analysis and analyzed data; M.S. and M.K. performed staging of biopsy specimens by histological activity index (HAI); H.N. conceived and designed the study, and supervised all aspects of the work; and all authors discussed the results and implications, and commented on the paper.

Additional information

Supplementary information accompanies this paper at http://www.nature.com/scientificreports

Competing financial interests: The authors declare no competing financial interests.

How to cite this article: Kuno, A. *et al.* A serum "sweet-doughnut" protein facilitates fibrosis evaluation and therapy assessment in patients with viral hepatitis. *Sci. Rep.* **3**, 1065; DOI:10.1038/srep01065 (2013).

Evaluation of the Mean and Entropy of Apparent Diffusion Coefficient Values in Chronic Hepatitis C: Correlation with Pathologic Fibrosis Stage and Inflammatory Activity Grade[1]

Kiminori Fujimoto, MD, PhD
Tatsuyuki Tonan, MD
Sanae Azuma, MD
Masayoshi Kage, MD, PhD
Osamu Nakashima, MD, PhD
Takeshi Johkoh, MD, PhD
Naofumi Hayabuchi, MD, PhD
Koji Okuda, MD, PhD
Takumi Kawaguchi, MD, PhD
Michio Sata, MD, PhD
Aliya Qayyum, MBBS

Purpose: To determine whether mean and entropy apparent diffusion coefficient (ADC) values obtained at diffusion-weighted (DW) magnetic resonance (MR) imaging can help detect and stage histopathologic liver fibrosis and grade inflammation activity in patients with chronic hepatitis C.

Materials and Methods: This retrospective study was approved by the institutional review board, and the requirement for informed consent was waived. The study included 55 patients with focal hepatic lesions and either chronic hepatitis C (n = 43) or normal hepatic function (control subjects) (n = 12). Mean and entropy of volume histograms were generated in four cubic regions of interest placed in the right hepatic lobe of ADC map images, which were obtained at echo-planar DW MR imaging (gradient factor b values of 0 and 1000 sec/mm^2). These two parameters (mean and entropy ADC) were compared by using METAVIR histopathologic liver fibrosis and inflammatory activity scores. Statistical analysis was performed with the Kruskal-Wallis test and receiver operating characteristic curves.

Results: The mean ADC decreased with an increase in the fibrosis stage or inflammatory activity grade, and the entropy ADC increased with an increase in the fibrosis stage or inflammatory activity grade ($P < .001$ for all comparisons, Kruskal-Wallis test). The area under the receiver operating characteristic curve (A_z) for the mean ADC was statistically significant in the differentiation of fibrosis stage or inflammatory activity grade (A_z, 0.807–0.926; $P < .001$ for all comparisons). Entropy of ADC was helpful for classifying normal from abnormal fibrosis stage or inflammatory activity grade (A_z for both parameters, 0.937; $P < .001$).

Conclusion: Assessment of a combination of mean ADC and entropy ADC in patients with chronic hepatitis C is more accurate for predicting pathologic hepatic fibrosis stage and inflammatory activity grade and helpful for detecting early fibrotic or inflammatory activity when compared with assessment of mean ADC alone.

[1] From the Departments of Radiology (K.F., T.T., S.A., N.H.), Diagnostic Pathology (M.K.), Pathology (O.N.), Surgery (K.O.), and Digestive Disease Information and Research (T.K., M.S.), Kurume University School of Medicine, 67 Asahi-machi, Kurume, 830-0011 Japan; Center for Diagnostic Imaging, Kurume University Hospital, Kurume, Japan (K.F.); Department of Radiology, Kinki Central Hospital of Mutual Aid Association of Public School Teachers, Itami, Japan (T.J.); and Department of Radiology, University of California–San Francisco, San Francisco, Calif (A.Q.).
Received April 27, 2010; revision requested June 18; revision received August 16; accepted September 8; final version accepted October 1. **Address correspondence to** K.F. (e-mail: *kimichan@med.kurume-u.ac.jp*).

It is estimated that approximately 400 million people worldwide are infected with the hepatitis C virus (1), with chronic infection in 75%–85% of patients. Once a diagnosis of chronic hepatitis C virus infection is established, cirrhosis develops within 10–20 years in approximately 20% of patients (2). Approximately 50% of patients with chronic hepatitis C fail to achieve a sustained virologic response to standard therapy with PEGylated interferon and ribavirin (3). Disease progression, which may lead to hepatic decompensation, hepatocellular carcinoma, and death, is particularly common in these patients (4,5).

The severity of liver inflammation and fibrosis in patients with chronic hepatitis C is important to consider when making therapeutic decisions and is a useful prognostic indicator. Liver biopsy is the current reference standard used in the assessment of hepatic necroinflammation and fibrosis (6). Several histologic scoring systems are used to evaluate chronic viral hepatitis (7–10). Of these, the METAVIR scoring system was specially designed for determining hepatic fibrosis stage in patients with chronic hepatitis C (10,11). The current focus in clinical practice, however, has shifted from diagnosis alone to risk stratification and disease monitoring (12,13). Liver biopsy is invasive, with a recognized morbidity and mortality, and as such repeated biopsy for the purpose of monitoring disease progression is not the best option. Furthermore, liver biopsies have several inherent limitations, such as sampling error and interobserver variability (6).

Several noninvasive techniques, including biochemical and hematologic tests, a scoring system using a combination of clinical and laboratory tests, ultrasonography (US)–based transient elastography (6,14), and magnetic resonance (MR) imaging (15–24), have been evaluated. Among these, diffusion-weighted (DW) MR imaging has shown promise in the detection and quantification of hepatic fibrosis (18–24) but has not yet been validated as a marker for pathologic hepatic necroinflammation. To our knowledge, semiquantitative analysis of DW MR imaging in the assessment of liver fibrosis has mainly been evaluated by determining the mean apparent diffusion coefficient (ADC) values of regions of interest in liver parenchyma, but volume histogram analyses have not been evaluated. Entropy describes the variation in a volume histogram of ADC and has been shown to have clinical utility for evaluating morphologic changes of organ tissues outside the abdomen (25,26). We postulated that the mean hepatic ADC values and the entropy of hepatic ADC (entropy ADC) values would be helpful for evaluating the alteration in hepatic parenchyma in chronic hepatitis C.

The purpose of this study was to determine whether the mean and entropy ADC values obtained with DW MR imaging can help detect and stage histopathologic liver fibrosis and grade inflammatory activity in patients with chronic hepatitis C.

Advance in Knowledge

- In patients with chronic hepatitis C, entropy of apparent diffusion coefficient (ADC) values might be a sensitive marker for the detection of early hepatic inflammatory activity (median entropy ADC value was 1.23 for an inflammatory activity score of A0 [no activity] and ranged from 1.48 to 1.57 for inflammatory activity scores of A1–A3 [mild to severe activity]) and fibrosis stage (median entropy ADC value was 1.24 for grade F0 fibrosis [no fibrosis] and ranged from 1.36 to 1.64 for grades F1–F4 fibrosis [minimal fibrosis to cirrhosis]).

Implication for Patient Care

- Evaluation of the mean and entropy of liver ADC values obtained with diffusion-weighted MR imaging is a noninvasive method for assessing liver fibrosis stage and inflammatory activity grade and might be used to differentiate early from advanced chronic liver disease; its noninvasiveness allows for repeat performance.

Materials and Methods

Patients

The institutional review board approved this retrospective study and waived the requirement to obtain patient approval or informed consent for the retrospective review of their records and images, which complied with the principles of the Declaration of Helsinki (2008 version) of the World Medical Association (27).

We retrospectively reviewed the medical records and MR images from all patients who underwent assessment of suspected focal hepatic lesions at our institution between June 2006 and May 2007 and who fulfilled the following inclusion criteria: *(a)* patients underwent DW MR imaging, *(b)* pathologic specimens obtained at liver biopsy were adequate for determining the METAVIR score, and *(c)* patients had either chronic active hepatitis C or absence of hepatic dysfunction or viral hepatitis. The patients with an absence of hepatic dysfunction or viral hepatitis were used as control subjects. Chronic active hepatitis C was defined as an established diagnosis of chronic hepatitis C virus infection with detectable anti–hepatitis C virus antibodies and detectable serum

Published online before print
10.1148/radiol.10100853

Radiology 2011; 258:739–748

Abbreviations:
ADC = apparent diffusion coefficient
A_z = area under the receiver operating characteristic curve
CI = confidence interval
DW = diffusion weighted
IQR = 25th to 75th percentile of the interquartile range

Author contributions:
Guarantors of integrity of entire study, K.F., T.T., M.K.; study concepts/study design or data acquisition or data analysis/interpretation, all authors; manuscript drafting or manuscript revision for important intellectual content, all authors; manuscript final version approval, all authors; literature research, K.F., T.T., M.K., T.J., T.K.; clinical studies, K.F., T.T., S.A., M.K., O.N., T.J., N.H., K.O., T.K., M.S.; statistical analysis, K.F.; and manuscript editing, K.F., A.Q.

Potential conflicts of interest are listed at the end of this article.

hepatitis C virus RNA in conjunction with serum aminotransferase levels that remained abnormally high for more than 6 months. Patients were excluded if they had *(a)* a life-threatening extrahepatic condition and *(b)* other causes of chronic liver disease (eg, hepatitis B virus, excessive alcohol consumption [>30 g per day], hemochromatosis, autoimmune hepatitis, Wilson disease, α_1-antitrypsin deficiency, primary sclerosing cholangitis, or primary biliary cirrhosis).

We identified 84 patients who underwent DW MR imaging and METAVIR scoring at our institution. Twenty-nine of those 84 patients were excluded because their chronic liver disease was due to a cause other than the hepatitis C virus (hepatitis B virus in 17 patients and excessive alcohol consumption in 12). Therefore, our final patient population consisted of 55 subjects, including 43 patients with chronic hepatitis C and 12 control subjects without hepatic dysfunction or viral hepatitis. Patients ranged in age from 34 to 83 years (median age, 65 years) and included 35 men and 20 women. The median patient age was 63 years (25th to 75th percentile of the interquartile range [IQR], 59–73 years) for men and 69 years (IQR, 55–72 years) for women. There was no statistically significant difference in age distribution according to sex ($P = .255$, Mann-Whitney U test).

In 48 of the 55 patients (36 patients with chronic hepatitis C and the 12 control subjects), pathologic assessment of the liver was performed by means of surgical biopsy at resection of the focal hepatic lesions (eg, hepatocellular carcinoma or hepatic metastases). In seven of the 55 patients, pathologic assessment of the liver was performed by means of US-guided biopsy with a 17-gauge core biopsy needle. The median interval between DW MR imaging and surgical or core liver biopsy was 7 days (range, 1–14 days).

MR Imaging Techniques and Interpretation

MR imaging was performed at a field strength of 1.5 T (Magnetom Symphony Advanced; Siemens, Erlangen, Germany) with use of a body phased-array coil.

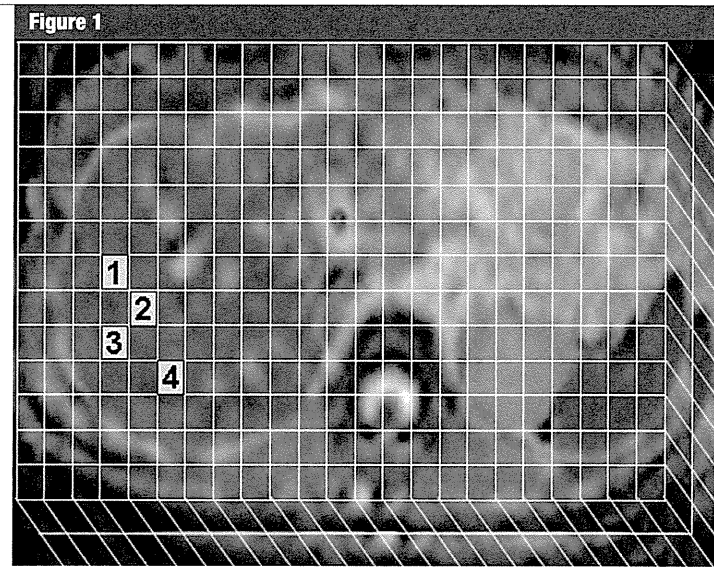

Figure 1: Image illustrates the method used to measure regions of interest on an ADC map. With use of computer software (developed in-house by authors), two independent observers freely and easily selected a region of interest by clicking a mesh unit on the right hepatic lobe of an ADC map image while avoiding the large vessels, focal hepatic lesions, or artifacts. Four cubic regions of interest (3.6 cm^3, approximately 36 voxels) were chosen for liver parenchyma. Numbers on image are regions of interest.

After routine T1- and T2-weighted imaging was performed for the assessment of focal hepatic lesions, a series of respiratory-triggered DW MR images was obtained in all patients.

DW MR imaging was performed in the transverse plane by combining single-shot spin-echo echo-planar imaging with a chemical shift–selective pulse. The imaging parameters for DW MR imaging were as follows: repetition time, 2000 msec; echo time, 81 msec; directions of the motion-probing gradient, three orthogonal axes; gradient factor b values of 0 and 1000 sec/mm^2; 2170-Hz per pixel bandwidth; 350-mm field of view; 128 × 88 rectangular matrixes; 9-mm-thick sections; 1-mm intersection gap; four signals acquired; and acquisition time of approximately 1 minute 30 seconds.

Liver ADC was calculated by using the following equation: $ADC = (-1/b) \times \ln (S_b/S_0)$, where b is the diffusion-sensitizing factor (b value), and S_b and S_0 the signal intensity with and without diffusion weighting, respectively. ADC maps were constructed according to this equation on the basis of a voxelwise calculation.

All regions of interest were determined by two independent observers (T.T. and S.A., with 12 and 8 years of experience, respectively) by using plug-in software developed in-house by two of the authors (K.F. and T.J.) (Fig 1). The two observers were abdominal radiologists who knew that all patients in the study had focal hepatic lesions but were blinded to the other clinical information. Four separate cubic regions of interest (3.6 cm^3, approximately 36 voxels) were manually placed in the anterior and posterior segments of the right hepatic lobe at the level of the porta hepatis (whenever possible) on the calculation ADC maps; care was taken to avoid focal lesions, major vascular structures, and artifacts such as chemical shifts, magnetic susceptibility, and cardiac motion. The regions of interest were drawn in the right hepatic lobe to approximate the regions expected to be sampled for histologic examination.

The entropy ADC values of the selected regions of interest, which were calculated by using the volume histogram method (24,25), were obtained automatically from the same plug-in software. Entropy describes the variation in an ADC histogram such that a large variation in hepatic ADC is associated with larger entropy values.

The histogram entropy was calculated as follows:

$$\text{Entropy} = \sum(-p_i)\log(p_i),$$

where p_i represents the probability of ADC value in the image and is calculated by dividing the number of voxels in each ADC value by the number of voxels in all ADC values.

Therefore, ADC values were recorded as the mean and entropy ADC of the volume histogram obtained from the selected regions of interest.

Assessment of Pathologic Specimens

Resected liver specimens (n = 48) and liver biopsy specimens (n = 7) were fixed in formalin, embedded in paraffin, and stained with hematoxylin and eosin. All specimens (n = 55) were retrospectively reviewed independently by two pathologists (M.K. and O.N., with 34 and 26 years of experience, respectively, and subspecialty expertise in liver pathology). The pathologists were blinded to clinical and imaging data.

The fibrosis stage and the necroinflammatory activity grade were evaluated semiquantitatively by using the METAVIR scoring system (9,13,20). Fibrosis was graded on a scale of 0 to 4, as follows: F0 = no fibrosis, F1 = portal fibrosis without septa, F2 = portal fibrosis and few septa, F3 = numerous septa without cirrhosis, and F4 = cirrhosis. The necroinflammatory activity score was graded on a scale of 0 to 3, as follows: A0 = no activity, A1 = mild activity, A2 = moderate activity, and A3 = severe activity. After calculating the κ values for interobserver agreement on the basis of the independent readings, any cases in which the final fibrosis stage or activity grade differed between the two pathologists were reevaluated and scored in consensus.

Statistical Analysis

The mean and entropy ADC values of the two independent observers' measurements were compared with the Bland-Altman method (28,29). The coefficients of repeatability were calculated as 1.96 times the standard deviation of the differences between the two measurements made by the two observers. The linear correlation coefficient (r value) of each difference of measurement was calculated by using Pearson linear regression analysis, and the estimated bias (ie, the mean difference between two observers' measurements) was assessed.

Agreement between the two pathologists with regard to the fibrosis stage and inflammatory activity grade was assessed by using κ statistics (30) with use of the diagnoses made before agreement by consensus. The strength of the interobserver agreement indicated with κ values was classified as follows: poor, $\kappa < 0.0$; slight, κ = 0.0–0.20; fair, κ = 0.21–0.40; moderate, κ = 0.41–0.60; substantial, κ = 0.61–0.80; and almost perfect, κ = 0.81–1.00 (31). The relationship between the fibrosis stage and inflammatory activity grade in patients with chronic hepatitis C was assessed by using the Spearman correlation test.

The Kruskal-Wallis test was used to determine the statistical significance of intergroup differences in the pathologic scores with mean and entropy ADC. In case of statistical significance, multiple pairwise comparisons were conducted with the Mann-Whitney U test with Bonferroni correction.

The diagnostic performance of mean or entropy ADC in predicting the fibrotic stage or inflammatory activity grade was assessed with use of the area under the receiver operating characteristic curve (A_z) (32). Sensitivity, specificity, positive and negative predictive values, and positive and negative likelihood ratios (33,34) for the classification of F0 versus F1–F4 fibrosis (score ≥F1); F0 and F1 versus F2–F4 fibrosis (score ≥F2); F0–F2 versus F3 and F4 fibrosis (score ≥F3); or F0–F3 versus F4 fibrosis (score = F4) and for the classification of A0 versus A1–A3 activity (grade ≥A1); A0 and A1 versus A2 and A3 activity (grade ≥A2); or A0–A2 versus A3 activity (grade = A3) were calculated with standard formulas according to the values of these indexes and with varied index values that indicated positive differentiation (ie, threshold values).

All analyses were performed with statistical software (SPSS, version 12.0J; SPSS, Chicago, Ill), and $P < .05$ was considered indicative of a statistically significant difference.

Results

Interobserver Agreement

There was no significant difference between measurements made by the two observers for the two parameters; the interclass Pearson correlation coefficients were 0.98 (95% confidence interval [CI]: 0.95, 1.0) for mean ADC and 0.97 (95% CI: 0.94, 1.0) for entropy ADC; the mean difference (±standard deviation) was −0.004 ± 0.05 for mean ADC and −0.013 ± 0.037 for entropy ADC; and the coefficients of repeatability were 0.100 for mean ADC and 0.072 for entropy ADC. Bland-Altman plots with 95% limits of agreement for mean and entropy ADC are shown in Figure 2a and Figure 2b, respectively. There was no proportional bias or fixed bias in each Bland-Altman plot for the two parameters.

There was substantial agreement between the two independent pathologists with regard to fibrosis stage (κ = 0.73; 95% CI: 0.59, 0.86) and inflammatory activity grade (κ = 0.74; 95% CI: 0.60, 0.88). None of the 12 control subjects had any signs of fibrosis or inflammatory activity because they did not have hepatic impairment. At the consensus reading, stage F0 fibrosis was diagnosed in 12 of the 55 patients (22%), stage F1 fibrosis in nine (16%), stage F2 fibrosis in 11 (20%), stage F3 fibrosis in 11 (20%), and stage F4 fibrosis in 12 (22%), showing a homogeneous distribution of fibrosis stages. The inflammatory activity grade was A0 in 12 of the 55 patients (22%), A1 in 13 (24%), A2 in 17 (31%), and A3 in 13 (24%). In the 43 patients with chronic hepatitis C, a significant correlation

Figure 2

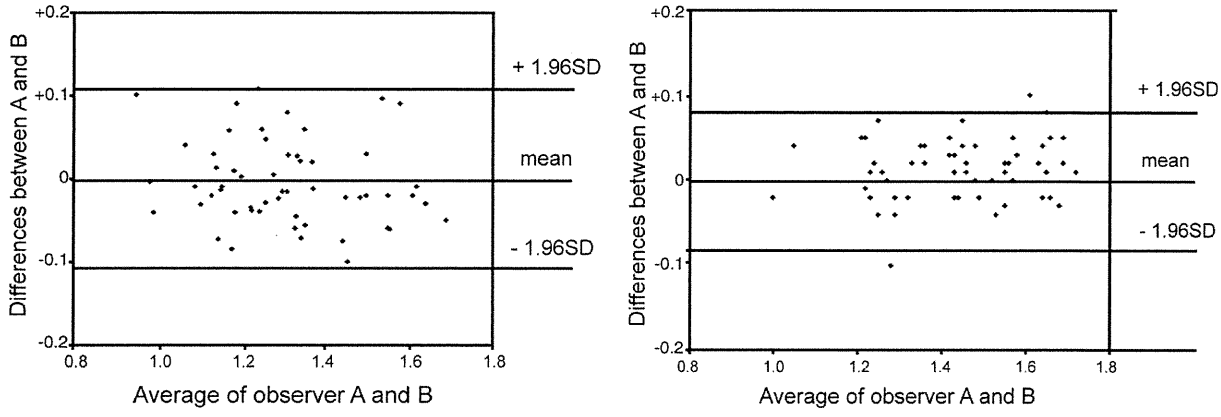

Figure 2: Bland-Altman plots depict measurements of **(a)** mean ADC (in $\times 10^{-3}$ mm²/sec) and **(b)** entropy ADC in liver parenchyma, demonstrating good interobserver agreement and lack of proportional bias or fixed bias. The average of the measurements made by the two observers is plotted against the difference between the measurements made by the two observers. The thin lines represent the mean value of all differences between the two observers, and the thick lines represent the 95% limits of agreement. *SD* = standard deviation.

was observed between the final fibrosis score and the final inflammatory activity grade ($r = 0.46$, $P = .002$, Spearman correlation test).

Relationship between ADC Parameters and Pathologic Fibrosis Stage

The median mean ADC values according to fibrosis stage were as follows: F0, 1.53×10^{-3} mm²/sec (IQR, $1.35–1.60 \times 10^{-3}$ mm²/sec); F1, 1.45×10^{-3} mm²/sec (IQR, $1.34–1.51 \times 10^{-3}$ mm²/sec); F2, 1.29×10^{-3} mm²/sec (IQR, $1.23–1.34 \times 10^{-3}$ mm²/sec); F3, 1.17×10^{-3} mm²/sec (IQR, $1.14–1.25 \times 10^{-3}$ mm²/sec); and F4, 1.15×10^{-3} mm²/sec (IQR, $1.01–1.26 \times 10^{-3}$ mm²/sec) (Fig 3a). The median entropy ADC values according to fibrosis stage were as follows: F0, 1.24 (IQR, 1.21–1.27); F1, 1.36 (IQR, 1.30–1.49); F2, 1.46 (IQR, 1.35–1.55); F3, 1.55 (IQR, 1.45–1.61); and F4, 1.64 (IQR, 1.45–1.68) (Fig 3b).

The mean ADC decreased with an increase in the stage of liver fibrosis ($P < .001$, Kruskal-Wallis test; Fig 3a). Conversely, the entropy ADC increased with an increase in fibrosis stage ($P < .001$, Kruskal-Wallis test; Fig 3b).

For the mean ADC, there were statistically significant differences in the pairwise comparisons (with Bonferroni correction) of stages of liver fibrosis, as follows: F0 versus F2, $P = .01$; F0 versus F3, $P < .01$; F0 versus F4, $P < .01$; F1 versus F3, $P < .01$; F1 versus F4, $P < .01$; F2 versus F3, $P = .04$; and F2 versus F4, $P = .04$ (Fig 3a). For the entropy ADC, there were statistically significant differences in the pairwise comparisons (Bonferroni correction) of stages of liver fibrosis, as follows: F0 versus F1, $P < .01$; F0 versus F2, $P < .01$; F0 versus F3, $P < .01$; and F1 versus F4, $P = .04$ (Fig 3b).

Relationship between ADC Parameters and Pathologic Inflammatory Activity Grade

The median mean ADC values according to inflammatory activity grade were as follows: A0, 1.53×10^{-3} mm²/sec (IQR, $1.36–1.60 \times 10^{-3}$ mm²/sec); A1, 1.30×10^{-3} mm²/sec (IQR, $1.21–1.51 \times 10^{-3}$ mm²/sec); A2, 1.26×10^{-3} mm²/sec (IQR, $1.19–1.34 \times 10^{-3}$ mm²/sec); and A3, 1.15×10^{-3} mm²/sec (IQR, $1.04–1.22 \times 10^{-3}$ mm²/sec) (Fig 4a). The median entropy ADC values according to activity grade were as follows: A0, 1.23 (IQR, 1.21–1.27); A1, 1.48 (IQR, 1.43–1.64); A2, 1.44 (IQR, 1.33–1.55); and A3, 1.57 (IQR, 1.50–1.67) (Fig 4b).

The mean ADC decreased with an increase in the inflammatory activity grade ($P < .001$, Kruskal-Wallis test; Fig 4a), and the entropy ADC increased with an increase in the inflammatory activity grade ($P < .001$, Kruskal-Wallis test; Fig 4b).

The mean ADC significantly differed between activity grades A0 and A2 and between activity grades A0 and A3 ($P < .01$ for both comparisons, Bonferroni correction) (Fig 4a). The entropy ADC significantly differed between inflammatory activity grade A0 and activity grades A1, A2, and A3 ($P < .01$ for all comparisons, Bonferroni correction) (Fig 4b).

Receiver Operating Characteristic Analyses and Diagnostic Performances for Predicting Pathologic Fibrosis and Activity Scores

The A_z values for mean and entropy ADCs according to different fibrosis and inflammatory activity thresholds are shown in Tables 1 and 2. Optimal cutoff values for mean and entropy ADC, along with the respective diagnostic performances, are shown in Tables 3 and 4.

The A_z for mean ADC was larger than that for entropy ADC in the classification of fibrosis of grade F2 or higher, fibrosis of grade F3 or higher, and fibrosis of grade F4 (Table 1). In

Figure 3

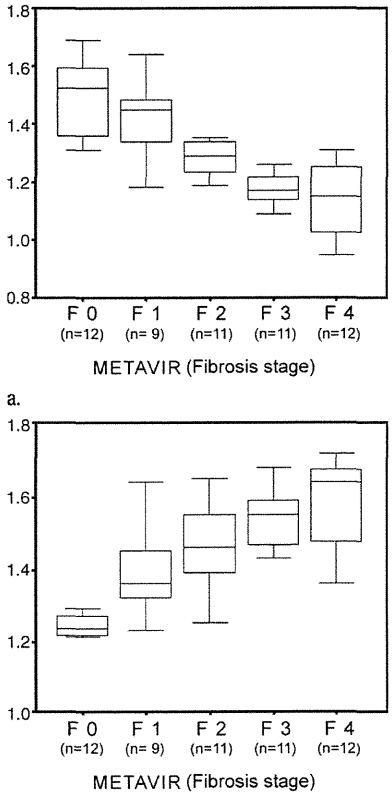

Figure 3: Box plots of **(a)** mean ADC (in $\times 10^{-3}$ mm²/sec) and **(b)** entropy ADC values in liver parenchyma according to METAVIR fibrosis score. The line in each box represents the median, and the horizontal boundaries of the boxes represent the first and third quartiles. The vertical error bars show the minimum and maximum values (range).

Figure 4

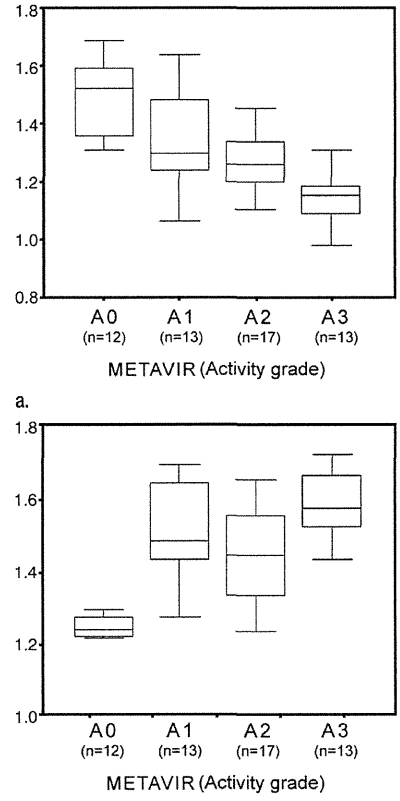

Figure 4: Box plots of **(a)** mean ADC (in $\times 10^{-3}$ mm²/sec) and **(b)** entropy ADC values in liver parenchyma according to METAVIR inflammatory activity score. The line in each box represents the median, and the horizontal boundaries of the boxes represent the first and third quartiles. The vertical error bars show the minimum and maximum values (range).

particular, diagnostic performances in the classification of grade F2 or higher fibrosis and grade F3 or higher fibrosis were quite good (cutoff values of 1.32 and 1.27 $\times$ 10^{-3} mm²/sec resulted in positive likelihood ratios of 9.0 and 5.6, respectively, and negative likelihood ratios of 0.16 and 0.15) (Table 3). Conversely, in the classification of fibrosis of grade F1 or higher, the A_z of entropy ADC was larger than that of mean ADC (Table 1). Thus, with regard to the diagnostic performance, entropy ADC was the most accurate parameter in the classification of grade F1 or higher fibrosis (cutoff value of 1.30 resulted in a positive likelihood ratio of 10.6 and negative likelihood ratio of 0.13). Similarly, the A_z of mean ADC was larger than that of entropy ADC in the classification of inflammatory activity of grade A2 or higher and grade A3 or higher. For inflammatory activity of at least grade A1, the A_z of entropy ADC was larger than that of mean ADC (Table 2). With regard to the diagnostic performance, entropy ADC was the most accurate parameter in the classification of inflammatory activity of grade A1 or higher (cutoff value of 1.30 resulted in a positive likelihood ratio of 10.9 and negative likelihood ratio of 0.10), and mean ADC was a relatively significant predictor for classification of grade A3 inflammatory activity (cutoff value of 1.19 $\times$ 10^{-3} mm²/sec resulted in a positive likelihood ratio of 4.6 and negative likelihood ratio of 0.28) (Table 4).

Discussion

Early studies assessing the relationship between hepatic fibrosis stage and ADC values in the liver reported that a significant correlation was not achieved when using low *b* values (eg, 0–128 sec/mm² and 50–400 sec/mm²) (15,18,19) because DW MR imaging with a low *b* value was influenced by perfusion contamination. Taouli et al (20) reported that the ADC value acquired from *b* values of at least 500 sec/mm² showed a significant correlation with the liver fibrosis stage and that the ADC value with a combination of *b* values of 0–1000 sec/mm² showed the highest significant correlation with fibrosis stage. On the basis of the study of combined ADC measurement with multiple *b* values (0, 200, 400, 800 sec/mm²), Luciani et al (35) reported that ADC changes observed in liver cirrhosis (METAVIR fibrosis score, F4) were more reflective of an alteration in microperfusion than of true diffusion. Although the use of multiple *b* values (intravoxel incoherent motion) may be helpful for differentiating the relative effect of altered microperfusion from that of true diffusion due to increased barriers to water movement, as suggested by Luciani et al, our results are consistent with those of other studies (15,20,21) that demonstrated that liver ADC derived from a combination of *b* values of 0 and 1000 sec/mm² is helpful for predicting hepatic fibrosis. The different correlations of ADC parameters and pathologic findings in our study compared with that of Luciani et al (35) may be explained in part by different patient populations; the patient population in the study by Luciani et al consisted of patients with cirrhosis (12 patients

with grade F4 fibrosis). Further studies (including those performed in patients with chronic hepatitis with a fibrosis score lower than F4) are needed to confirm these findings and shed light on the exact mechanism of diffusion changes observed in liver fibrosis (22).

Previous studies have reported a range of liver ADC sensitivities of 0.74–0.89 and specificities of 0.73–0.87 in the detection of moderate fibrosis (stage F2 or higher) (15,19,21). These findings concur with our observation of mean ADC sensitivity (0.85) and specificity (0.91); however, we observed a greater specificity (0.92) with entropy ADC when including even early liver fibrosis.

Although Lewin et al (15) and Taouli et al (21) reported weak negative correlations between ADC values and the degree of necroinflammation, with a sensitivity of 0.75 and a specificity of 0.78, we observed a stronger negative correlation between mean ADC and inflammatory activity grade (sensitivity, 0.81; specificity, 0.83). In addition, entropy, which is a measure of the variability in the volume histogram analyses of the ADC values, showed a greater correlation with the fibrosis stage and inflammatory activity grade than did mean ADC, with a sensitivity of 0.91 and a specificity of 0.92 in the detection of inflammation.

In patients with chronic hepatitis C, a significant correlation between the pathologic fibrosis stage and the inflammatory activity grade is well known (36,37). Our results are consistent with those results and indicate that fibrosis tends to evolve as necroinflammation becomes more pronounced in chronic hepatitis C. Although the Spearman coefficient value was relatively low (r = 0.46), this trend may be one of the reasons why liver ADC showed an inverse correlation with both fibrosis stage and inflammatory activity grade. The possible biologic implications of a reduced mean ADC value and an increased entropy ADC value with increasing fibrosis stage and inflammation are intracellular alterations, changes of cellular composition, and decreased interstitial fluids according to the fibrosis stage and inflammatory activity grade.

Table 1

A_z Values for Mean and Entropy ADC according to METAVIR Fibrosis Score

Parameter	≥F1	≥F2	≥F3	F4
Mean ADC	0.889 (0.799, 0.978)	0.925 (0.851, 0.999)	0.926 (0.859, 0.993)	0.842 (0.730, 0.954)
Entropy ADC	0.937 (0.855, 1.0)	0.882 (0.787, 0.978)	0.855 (0.759, 0.950)	0.815 (0.675, 0.954)

Note.—Data are given as mean A_z values. Numbers in parentheses are 95% CIs. $P < .001$ for all comparisons.

Table 2

A_z Values for Mean and Entropy ADC according to METAVIR Activity Grade

Parameter	≥A1	≥A2	A3
Mean ADC	0.889 (0.799, 0.978)	0.807 (0.690, 0.925)	0.842 (0.722, 0.961)
Entropy ADC	0.937 (0.855, 1.0)	0.697 (0.554, 0.841)*	0.808 (0.691, 0.925)

Note.—Data are given as mean A_z values. Numbers in parentheses are 95% CIs. Except where indicated, $P < .001$.

* $P = .012$.

Our data highlight entropy ADC as a sensitive marker of overall hepatic damage that strongly correlated to pathologic fibrosis stage and inflammatory activity grade in patients with chronic hepatitis C. The most prominent finding of our study is the difference in entropy ADC values between patients without any signs of fibrosis (stage F0) and those with fibrosis of any pathologic stage (stages F1–F4) and between patients without inflammatory activity (grade A0) and those with any grade of inflammatory activity (grades A1–A3). Although other studies using entropy have not been performed in the abdomen, studies in patients with multiple sclerosis have shown that entropy can help measure macroscopic and microscopic tissue changes in the brain (25,26); neurologic damage has been reportedly associated with increased heterogeneity of signal intensities at DW imaging of the brain (25,26). As the distribution of these signal intensities becomes more heterogeneous (and the image therefore more random), entropy increases. Histopathologically, early fibrosis and inflammatory activity in chronic viral hepatitis demonstrate mild portal fibrosis and mild piecemeal necrosis and/or lobular necrosis (9,37) in addition to vascular changes (damage and disappearance of some branches of the portal veins) (38). In viral hepatitis, liver fibrosis begins in the portal triads and extends into the surrounding hepatic parenchyma. Thickening and lengthening of the fibrous septa results in the formation of fibrous bridges that link adjacent portal triads and central veins. With progressive liver injury, the bridges continue to enlarge and coalesce and eventually divide the liver into rounded islands of hepatic parenchyma (regenerative nodules) surrounded by fibrosis tissue. The change in tissue composition and architecture may be expected to increase barriers to water movement. The deposition of fibrous tissue leads to a reduction in the size or obliteration of small venules, with a resultant increase in portal venous pressure and consequent compensatory increased arterial blood flow. Changes in regional liver perfusion may have contributed to the increase in entropy ADC we observed in the early stages of liver disease. Infiltration of inflammatory cells into the liver interstitial tissue would also be expected to reduce water movement and increase liver ADC with regional variation. Regardless of early stage and grade, when these changes are combined, it causes the liver to go to a structure with an unstable architectural state according to chronic liver injury, from a normal structure with orderly normal tissue. The observation of increased liver entropy ADC depicted by means of the increased variability of ADC at

Table 3

Performance of Mean and Entropy ADC in the Prediction of METAVIR Fibrosis Score according to Cutoff Values

Parameter*	≥F1	≥F2	≥F3	F4
Cutoff mean ADC ($\times 10^{-3}$ mm²/sec)	1.35	1.32	1.27	1.23
Sensitivity	0.79 (0.64, 0.90)	0.85 (0.69, 0.95)	0.87 (0.66, 0.97)	0.75 (0.43, 0.95)
Specificity	0.83 (0.52, 0.98)	0.91 (0.70, 0.99)	0.84 (0.67, 0.95)	0.72 (0.56, 0.85)
PPV	0.94 (0.81, 0.99)	0.94 (0.79, 0.99)	0.80 (0.59, 0.93)	0.43 (0.22, 0.66)
NPV	0.53 (0.29, 0.76)	0.79 (0.58, 0.93)	0.90 (0.73, 0.98)	0.91 (0.76, 0.98)
Positive LR	4.7 (1.8, 16.7)	9.0 (3.2, 30.7)	5.6 (2.9, 9.4)	2.7 (1.4, 3.8)
Negative LR	0.25 (0.19, 0.47)	0.16 (0.11, 0.31)	0.15 (0.06, 0.36)	0.35 (0.12, 0.76)
Cutoff entropy ADC	1.30	1.43	1.48	1.58
Sensitivity	0.88 (0.72, 0.97)	0.82 (0.65, 0.93)	0.74 (0.52, 0.90)	0.67 (0.35, 0.090)
Specificity	0.92 (0.62, 0.99)	0.86 (0.64, 0.97)	0.78 (0.61, 0.89)	0.88 (0.75, 0.96)
PPV	0.97 (0.83, 0.995)	0.90 (0.74, 0.98)	0.71 (0.49, 0.87)	0.62 (0.31, 0.86)
NPV	0.69 (0.41, 0.89)	0.75 (0.53, 0.90)	0.81 (0.63, 0.93)	0.90 (0.77, 0.97)
Positive LR	10.6 (2.7, 58.8)	5.8 (2.5, 15.5)	3.4 (1.8, 6.1)	5.7 (2.4, 12.0)
Negative LR	0.13 (0.10, 0.25)	0.21 (0.13, 0.38)	0.33 (0.18, 0.61)	0.38 (0.18, 0.69)

Note.—Numbers in parentheses are 95% CIs.

* LR = likelihood ratio, NPV = negative predictive value, PPV = positive predictive value.

Table 4

Performance of Mean and Entropy ADC in the Prediction of METAVIR Inflammatory Activity Score according to Cutoff Values

Parameter*	≥A1	≥A2	A3
Cutoff mean ADC value ($\times 10^{-3}$ mm²/sec)	1.35	1.28	1.19
Sensitivity	0.81 (0.67, 0.92)	0.73 (0.54, 0.88)	0.77 (0.46, 0.95)
Specificity	0.83 (0.52, 0.98)	0.80 (0.59, 0.93)	0.83 (0.69, 0.93)
PPV	0.95 (0.82, 0.99)	0.81 (0.62, 0.94)	0.59 (0.33, 0.82)
NPV	0.56 (0.31, 0.78)	0.71 (0.51, 0.87)	0.92 (0.79, 0.98)
Positive LR	4.8 (1.8, 17.1)	3.7 (1.8, 7.9)	4.6 (2.3, 7.4)
Negative LR	0.22 (0.16, 0.43)	0.33 (0.21, 0.58)	0.28 (0.10, 0.60)
Cutoff entropy ADC value	1.30	1.43	1.51
Sensitivity	0.91 (0.78, 0.97)	0.73 (0.54, 0.88)	0.77 (0.46, 0.95)
Specificity	0.92 (0.62, 0.99)	0.60 (0.39, 0.79)	0.76 (0.61, 0.88)
PPV	0.98 (0.87, 0.99)	0.69 (0.50, 0.84)	0.50 (0.27, 0.73)
NPV	0.73 (0.45, 0.92)	0.65 (0.43, 0.84)	0.91 (0.77, 0.98)
Positive LR	10.9 (2.8, 59.7)	1.8 (1.1, 3.0)	3.2 (1.7, 4.7)
Negative LR	0.10 (0.08, 0.22)	0.44 (0.23, 0.84)	0.30 (0.11, 0.67)

Note.—Numbers in parentheses are 95% CIs.

* LR = likelihood ratio, NPV = negative predictive value, PPV = positive predictive value.

volumetric histogram analysis may therefore be a potential biomarker that reflects increased heterogeneity of hepatic parenchyma in diffuse liver disease. Furthermore, entropy ADC may be more helpful than mean ADC alone for detecting early stage fibrosis and early inflammatory activity.

There are a few limitations to our study. First, the study was retrospective and involved a small number of patients. A prospective study with a substantially larger sample is needed to further validate our findings. Second, because the pathologic specimens were obtained at surgery for a hepatic mass or with core biopsy, exact mapping of pathologic findings and imaging was not possible. However, our study was targeted at evaluating diffuse hepatic disease rather than characterizing focal lesions. Third, DW MR imaging is susceptible to motion artifacts that may interfere with quantitative measurements. We used respiratory-triggered DW MR imaging to reduce respiratory artifacts. The use of mean ADC and volumetric acquisition for entropy ADC should result in averaging of signal intensities to provide some compensation for respiratory motion. In addition, all measurements were obtained in the right lobe of the liver because the left lobe exhibits greater motion-related artifact. However, core liver biopsy, which is often used as the standard for staging the severity of liver disease, is also performed from the right lobe of the liver. Fourth, we used a combination of *b* values of 0 and 1000 sec/mm² for DW imaging. Further studies using a combination of at least three *b* values might be needed.

In summary, our data suggest that the diagnostic performance of mean or entropy ADC for predicting pathologic stage or inflammatory grade is at least similar to that of other DW MR imaging studies (22); however, the combination of mean and entropy ADC may improve diagnostic performances, particularly in the detection of inflammatory activity in the liver.

In practical clinical use, the evaluation with mean and entropy ADC may have several advantages: *(a)* The noninvasive nature of the examination allows for repeat performance; *(b)* entropy ADC may be able to help differentiate normal from any abnormal fibrosis stage or abnormal inflammatory activity grade and, thus, may represent indexes at the initiation of treatment and of improvement after treatment; and *(c)* mean ADC may reflect abnormal fibrosis stage (especially ≥F2 and ≥F3) and, thus, may help determine disease severity and the effects of therapy performed to treat hepatic fibrosis.

In conclusion, our preliminary data suggest that mean and entropy ADC might be helpful for predicting pathologic hepatic fibrosis stage and inflammatory activity grade in patients with chronic hepatitis C.

Disclosures of Potential Conflicts of Interest: **K.F.** Financial activities related to the present article: none to disclose. Financial activities not related to the present article: none to disclose. Other relationships: none to disclose. **T.T.** Financial activities related to the present article: none to disclose. Financial activities not related to the present article: none to disclose. Other relationships: none to disclose. **S.A.** Financial activities related to the present article: none to disclose. Financial activities not related to the present article: none to disclose. Other relationships: none to disclose. **M.K.** Financial activities related to the present article: none to disclose. Financial activities not related to the present article: none to disclose. Other relationships: none to disclose. **O.N.** Financial activities related to the present article: none to disclose. Financial activities not related to the present article: none to disclose. Other relationships: none to disclose. **T.J.** Financial activities related to the present article: none to disclose. Financial activities not related to the present article: none to disclose. Other relationships: none to disclose. **N.H.** Financial activities related to the present article: none to disclose. Financial activities not related to the present article: none to disclose. Other relationships: none to disclose. **K.O.** Financial activities related to the present article: none to disclose. Financial activities not related to the present article: none to disclose. Other relationships: none to disclose. **T.K.** Financial activities related to the present article: none to disclose. Financial activities not related to the present article: none to disclose. Other relationships: none to disclose. **M.S.** Financial activities related to the present article: none to disclose. Financial activities not related to the present article: none to disclose. Other relationships: none to disclose. **A.Q.** Financial activities related to the present article: none to disclose. Financial activities not related to the present article: none to disclose. Other relationships: none to disclose.

References

1. Ezelle HJ, Markovic D, Barber GN. Generation of hepatitis C virus-like particles by use of a recombinant vesicular stomatitis virus vector. J Virol 2002;76(23):12325–12334.
2. Afdhal NH. The natural history of hepatitis C. Semin Liver Dis 2004;24(suppl 2):3–8.
3. Strader DB, Wright T, Thomas DL, Seeff LB; American Association for the Study of Liver Diseases. Diagnosis, management, and treatment of hepatitis C. Hepatology 2004;39(4):1147–1171.
4. Tsukuma H, Hiyama T, Tanaka S, et al. Risk factors for hepatocellular carcinoma among patients with chronic liver disease. N Engl J Med 1993;328(25):1797–1801.
5. Hofmann WP, Zeuzem S, Hepatitis C. Hepatitis C: new therapeutic strategies needed for advanced disease. Nat Rev Gastroenterol Hepatol 2009;6(6):325–327.
6. Manning DS, Afdhal NH. Diagnosis and quantitation of fibrosis. Gastroenterology 2008;134(6):1670–1681.
7. Batts KP, Ludwig J. Chronic hepatitis: an update on terminology and reporting. Am J Surg Pathol 1995;19(12):1409–1417.
8. Knodell RG, Ishak KG, Black WC, et al. Formulation and application of a numerical scoring system for assessing histological activity in asymptomatic chronic active hepatitis. Hepatology 1981;1(5):431–435.
9. Ishak K, Baptista A, Bianchi L, et al. Histological grading and staging of chronic hepatitis. J Hepatol 1995;22(6):696–699.
10. Intraobserver and interobserver variations in liver biopsy interpretation in patients with chronic hepatitis C. The French METAVIR Cooperative Study Group. Hepatology 1994;20(1 pt 1):15–20.
11. Rozario R, Ramakrishna B. Histopathological study of chronic hepatitis B and C: a comparison of two scoring systems. J Hepatol 2003;38(2):223–229.
12. Talwalkar JA, Yin M, Fidler JL, Sanderson SO, Kamath PS, Ehman RL. Magnetic resonance imaging of hepatic fibrosis: emerging clinical applications. Hepatology 2008;47(1):332–342.
13. Mallet V, Gilgenkrantz H, Serpaggi J, et al. Brief communication: the relationship of regression of cirrhosis to outcome in chronic hepatitis C. Ann Intern Med 2008;149(6):399–403.
14. Friedrich-Rust M, Wunder K, Kriener S, et al. Liver fibrosis in viral hepatitis: noninvasive assessment with acoustic radiation force impulse imaging versus transient elastography. Radiology 2009;252(2):595–604.
15. Lewin M, Poujol-Robert A, Boëlle PY, et al. Diffusion-weighted magnetic resonance imaging for the assessment of fibrosis in chronic hepatitis C. Hepatology 2007;46(3):658–665.
16. Lucidarme O, Baleston F, Cadi M, et al. Noninvasive detection of liver fibrosis: is superparamagnetic iron oxide particle–enhanced MR imaging a contributive technique? Eur Radiol 2003;13(3):467–474.
17. Aguirre DA, Behling CA, Alpert E, Hassanein TI, Sirlin CB. Liver fibrosis: noninvasive diagnosis with double contrast material–enhanced MR imaging. Radiology 2006;239(2):425–437.
18. Koinuma M, Ohashi I, Hanafusa K, Shibuya H. Apparent diffusion coefficient measurements with diffusion-weighted magnetic resonance imaging for evaluation of hepatic fibrosis. J Magn Reson Imaging 2005;22(1):80–85.
19. Sandrasegaran K, Akisik FM, Lin C, et al. Value of diffusion-weighted MRI for assessing liver fibrosis and cirrhosis. AJR Am J Roentgenol 2009;193(6):1556–1560.
20. Taouli B, Tolia AJ, Losada M, et al. Diffusion-weighted MRI for quantification of liver fibrosis: preliminary experience. AJR Am J Roentgenol 2007;189(4):799–806.
21. Taouli B, Chouli M, Martin AJ, Qayyum A, Coakley FV, Vilgrain V. Chronic hepatitis: role of diffusion-weighted imaging and diffusion tensor imaging for the diagnosis of liver fibrosis and inflammation. J Magn Reson Imaging 2008;28(1):89–95.
22. Taouli B, Koh DM. Diffusion-weighted MR imaging of the liver. Radiology 2010;254(1):47–66.
23. Girometti R, Furlan A, Esposito G, et al. Relevance of *b*-values in evaluating liver fibrosis: a study in healthy and cirrhotic subjects using two single-shot spin-echo echo-planar diffusion-weighted sequences. J Magn Reson Imaging 2008;28(2):411–419.
24. Huwart L, Sempoux C, Vicaut E, et al. Magnetic resonance elastography for the noninvasive staging of liver fibrosis. Gastroenterology 2008;135(1):32–40.
25. Benedict RH, Bruce J, Dwyer MG, et al. Diffusion-weighted imaging predicts cognitive impairment in multiple sclerosis. Mult Scler 2007;13(6):722–730.
26. Tavazzi E, Dwyer MG, Weinstock-Guttman B, et al. Quantitative diffusion weighted imaging measures in patients with multiple sclerosis. Neuroimage 2007;36(3):746–754.
27. WMA Declaration of Helsinki—Ethical Principles for Medical Research Involving Human Subjects. Amended by the 59th WMA General Assembly, Seoul, October 2008. World Medical Association. http://www.wma.net/en/30publications/10policies/b3/index.html. Updated October 22, 2008. Accessed January 10, 2010.
28. Bland JM, Altman DG. Statistical methods for assessing agreement between two methods of clinical measurement. Lancet 1986;1(8476):307–310.
29. Ludbrook J. Statistical techniques for comparing measurers and methods of measurement:

a critical review. Clin Exp Pharmacol Physiol 2002;29(7):527–536.

30. Kundel HL, Polansky M. Measurement of observer agreement. Radiology 2003;228(2):303–308.

31. Landis JR, Koch GG. The measurement of observer agreement for categorical data. Biometrics 1977;33(1):159–174.

32. DeLong ER, DeLong DM, Clarke-Pearson DL. Comparing the areas under two or more correlated receiver operating characteristic curves: a nonparametric approach. Biometrics 1988;44(3):837–845.

33. Jaeschke R, Guyatt GH, Sackett DL. Users' guides to the medical literature. III. How to use an article about a diagnostic test. B. What are the results and will they help me in caring for my patients? The Evidence-Based Medicine Working Group. JAMA 1994;271(9):703–707.

34. Fritz JM, Wainner RS, Wainner RS. Examining diagnostic tests: an evidence-based perspective. Phys Ther 2001;81(9):1546–1564.

35. Luciani A, Vignaud A, Cavet M, et al. Liver cirrhosis: intravoxel incoherent motion MR imaging—pilot study. Radiology 2008;249(3):891–899.

36. Yano M, Kumada H, Kage M, et al. The long-term pathological evolution of chronic hepatitis C. Hepatology 1996;23(6):1334–1340.

37. Kage M, Fujisawa T, Shiraki K, et al. Pathology of chronic hepatitis C in children. Child Liver Study Group of Japan. Hepatology 1997;26(3):771–775.

38. Hano H, Takasaki S. Three-dimensional observations on the alterations of lobular architecture in chronic hepatitis with special reference to its angioarchitecture for a better understanding of the formal pathogenesis of liver cirrhosis. Virchows Arch 2003;443(5):655–663.

Ann Surg Oncol
DOI 10.1245/s10434-013-3376-9

Annals of
SURGICAL ONCOLOGY
OFFICIAL JOURNAL OF THE SOCIETY OF SURGICAL ONCOLOGY

ORIGINAL ARTICLE – HEPATOBILIARY TUMORS

The Significance of Classifying Microvascular Invasion in Patients with Hepatocellular Carcinoma

Shuji Sumie, MD[1], Osamu Nakashima, MD[2], Koji Okuda[3], Ryoko Kuromatsu[1], Atsushi Kawaguchi, MD[4], Masahito Nakano, PhD[1], Manabu Satani, MD[1], Shingo Yamada, MD[1], Shusuke Okamura, MD[1], Maisa Hori, MD[1], Tatsuyuki Kakuma, PhD[4], Takuji Torimura, MD[1,5], and Michio Sata, MD[1]

[1]Division of Gastroenterology, Department of Medicine, Kurume University School of Medicine, Kurume, Fukuoka, Japan; [2]Department of Clinical Laboratory Medicine, Kurume University School of Medicine, Kurume, Fukuoka, Japan; [3]Division of Hepato-Biliary-Pancreatic Surgery, Kurume University School of Medicine, Kurume, Fukuoka, Japan; [4]Biostatistics Center, Kurume University School of Medicine, Kurume, Fukuoka, Japan; [5]Liver Cancer Research Division, Research Center for Innovative Cancer Therapy, Kurume University School of Medicine, Kurume, Fukuoka, Japan

ABSTRACT

Background. Microvascular invasion (MVI) has been recognized as a risk factor for outcome following curative resection in hepatocellular carcinoma (HCC). Because MVI can range from few to many invaded vessels, we evaluated the significance of MVI classification in this study.

Methods. Between January 1995 and December 2010, 207 consecutive patients who underwent curative resection for HCC within Milan criteria were included in this retrospective study. Patients were classified into mild and severe MVI groups based on the number of vessels invaded. This study evaluated whether MVI classification can help to predict recurrence and survival after curative resection.

Results. Of the total 207 patients, 103 (50 %) patients had no detectable MVI, whereas 59 (28 %) had mild MVI, and 45 (22 %) had severe MVI. Recurrence-free survival rates at 2 years for patients without MVI, with mild MVI, and severe MVI were 75.9, 47.2, and 32.7 %, respectively. Patients with severe MVI experienced a high frequency of fatal recurrence, such as multiple tumors, macroscopic vascular invasion, and extrahepatic metastasis after curative resection. Multivariate analysis revealed age, number of tumors, mild MVI, and severe MVI as independent predictors of recurrence-free survival. Disease-specific survival rates at 5 years for patients without MVI, with mild MVI, and severe MVI were 91.5, 70.4, and 51.4, respectively. Multivariate analysis also revealed cirrhosis, tumor size, mild MVI, and severe MVI as independent predictors of disease-specific survival.

Conclusions. We demonstrated that MVI classification can stratify HCC patients by different patterns of recurrence and risk of survival after curative resection.

Hepatocellular carcinoma (HCC) is one of the most common malignancies in the world. Recent advances in imaging procedures and surveillance programs for high-risk patients have led to increased detection of early-stage HCC, resulting in an increase in identification of patients in whom curative resection is possible.[1,2] However, the long-term survival of HCC patients remains unsatisfactory due to the high frequency of intra- and extrahepatic recurrences.[3,4] Vascular invasion (VI) has been recognized as a risk factor leading to early recurrence of HCC.[5–8] Moreover, the fatal recurrence in HCC patients with VI limits additional attempts at various curative therapies, such as liver resection and radiofrequency ablation (RFA), thereby contributing to poor survival.[9,10]

VI is generally classified using either macroscopic or microscopic findings. Macroscopic VI, such as a tumor thrombus in the major portal vein, is known to be a crucial risk factor for survival after liver resection or transplantation in HCC patients and is detectable by various imaging procedures.[11–14] Therefore, the presence of macroscopic VI is usually evaluated before treatment and is an important parameter that is included in the TNM, CLIP, JIS, and BCLC scoring systems and is used to determine treatment

First Received: 22 February 2013

S. Sumie, MD
e-mail: sumie_shyuuji@kurume-u.ac.jp

Published online: 20 November 2013

strategies in HCC patients.[10,15,16] In contrast, microscopic vascular invasion (MVI) is difficult to detect before initiation of HCC treatment, even if sophisticated imaging procedures are conducted during patient evaluation. Recently, many studies have reported that the presence of MVI is closely associated with outcome following liver resection or transplantation in HCC patients.[17–21] Our previous study also showed that MVI was an important strong risk factor for recurrence and survival following resection of HCC within the Milan criteria.[22] Therefore, MVI is as important as macroscopic VI and should be evaluated as a risk factor of patients with HCC. Moreover, the current definition of MVI encompasses a wide range of tumor invasion, from one to many microscopic vessels that are contiguous with the tumor. Thus, patients with MVI have been suggested to have a wide range of outcomes after resection. Consequently, the purpose of this study was to evaluate whether the classification of MVI based on number of vessels invaded affects tumor recurrence and survival after resection of HCC.

METHODS

Patients

Between January 1995 and December 2010, 256 patients underwent liver resection at the Kurume University School of Medicine and were diagnosed with HCC by histological findings. The following patients were excluded: (1) patients whose disease did not fulfill the Milan criteria (a single tumor $\leq$5 cm or $\leq$3 tumors each $\leq$3 cm); (2) patients with macroscopic VI; (3) patients with extrahepatic metastasis; (4) patients who underwent noncurative liver resection; and (5) patients who were diagnosed with combined hepatocellular and cholangiocellular carcinoma by histological findings. Of the total 256 patients, 49 patients having one or more of the above criteria were excluded, and the remaining 207 patients were retrospectively enrolled in this study. Patients included 162 males (78 %) and 45 females, with a median age of 66 (range 16–83) years. Overall, 147 patients (71 %) were positive for hepatitis C virus (HCV) infection and 46 patients (22 %) were positive for hepatitis B virus (HBV) infection. Liver cirrhosis was present in 81 patients (39 %). The median tumor size was 25 (range 12–50) mm, and 160 patients (77 %) had a solitary tumor. Various surgical procedures were classified as major or minor resections according to Couinaud's segment classification. Major resections (segmentectomy, sectorectomy, and lobectomy or greater) were performed in 123 patients, whereas minor resections (all other types of resection, including partial hepatectomy and subsegmentectomy) were performed in 84 patients.

Follow-Up and Endpoint

After surgical resection, each patient was followed carefully. Serum biochemistries, alpha-fetoprotein (AFP) levels, and des-gamma-carboxy prothrombin (DCP) levels were measured, and ultrasonography was performed monthly. Contrast-enhanced dynamic computed tomography (CT) was performed every 3 months until 6 months posttreatment and every 6 months thereafter. Magnetic resonance imaging (MRI) was performed as a supplemental examination. Recurrence was diagnosed based on the combined findings of these examinations with appearances typical of HCC. The endpoint of this study was the date of recurrence, death, or last follow-up visit; the closing date was December 2011. The median duration of follow-up was 54.4 (range 9.5–177.8) months.

Histopathological Evaluation

The resected liver specimens were cut into serial 2–3-mm thick slices and fixed in 10 % formalin to facilitate careful gross and histopathological examinations. Each of the liver slices was embedded in paraffin, cut into 4-mm sections, and stained with hematoxylin and eosin. Tumors were examined for maximum tumor size, MVI, intrahepatic micrometastasis, capsular formation, and histologic grade. Noncancerous liver parenchyma was inspected for evidence of cirrhosis. Histological grade was based on the criteria of the Edmondson-Steiner classification and the Liver Cancer Study Group of Japan.[23,24] Intrahepatic micrometastasis was defined as a satellite micronodule in the surrounding liver tissue that is isolated from the main tumor. MVI was defined as microscopic tumor invasion identified in the portal vein and hepatic vein of the surrounding liver tissue that is contiguous with the tumor edge. Moreover, we hypothesize that the extent of MVI may affect tumor recurrence and survival after resection, because MVI encompasses a wide range of tumor invasion. Therefore, in this study, we devised a novel classification of MVI based on number of invaded vessels and divided the patients with MVI into two groups as follows: patients in the mild MVI group had one to five invaded vessels, whereas patients in the severe MVI group had more than five invaded vessels. The number of MVI was counted in each nodule. If patients had multiple tumors, the tumor with the most number of invaded vessels was selected for the classification of MVI. These histopathological evaluations of the resected specimens were retrospectively performed by one experienced pathologist (O.N.). Typical examples of the two MVI types are shown in Fig. 1.

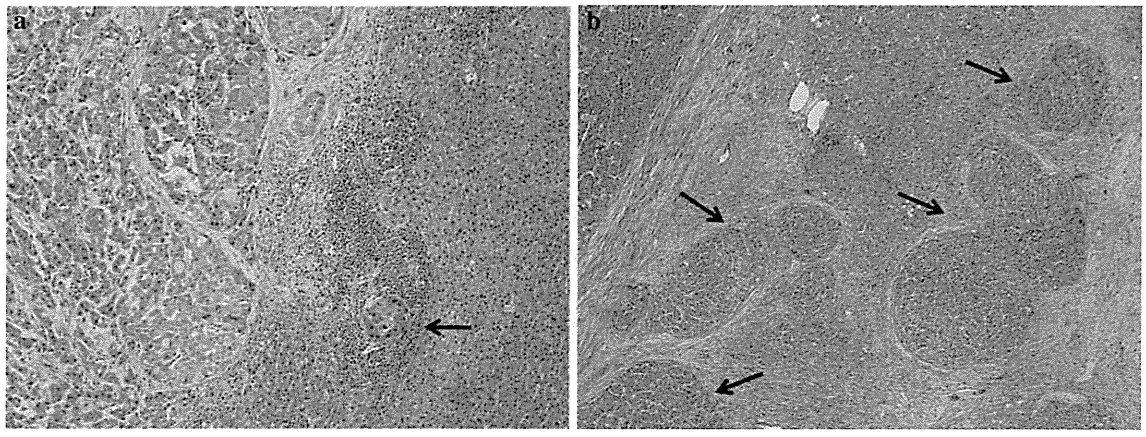

FIG. 1 Typical examples of the two microvascular invasion (MVI) types classified by number of vessels invasion. **a** mild MVI: peritumoral vessel invasion from one to five (hematoxylin–eosin, ×50). **b** severe MVI: peritumoral vessel invasion more than five (hematoxylin–eosin, ×20)

Statistical Analysis

Continuous variables were expressed as median (range). Comparison analysis among MVI grades was performed using the Chi square test for discrete variables and the Kruskal–Wallis test followed by Mann–Whitney *U* test with Bonferroni correction as a post hoc test for continuous variables. Recurrence-free survival and disease-specific survival were determined by Kaplan–Meier analysis, and differences between subgroups were compared with log-rank tests. A cause specific Cox proportional hazards model was used for univariate and multivariate analysis to identify separately any independent variables that were related to recurrence-free survival or disease-specific survival. The variables that were statistically significant by univariate analysis were included in a multivariate analysis. No interaction terms were considered, because the preanalysis showed the nonsignificance for the interaction. Data from these models were expressed as hazard ratio (HR) and 95 % confidence interval (95 % CI). All *P* values were two-tailed, and a level of <0.05 was considered to be statistically significant. Statistical analysis was performed by SPSS software version 20 (SPSS Inc., Chicago, IL, USA).

RESULTS

Comparison of Patient Characteristics Based on Grade of MVI and Predictors of Severe MVI

Clinicopathological characteristics of this study population stratified by grade of MVI are shown in Table 1. Of the total 207 patients, 103 (50 %) patients had no detectable MVI, whereas 59 (28 %) had mild MVI, and 45 (22 %) had severe MVI on pathologic examination. Patients with severe MVI had significantly higher elevated AFP and DCP levels compared with patients without MVI or with mild MVI. Patients with worse MVI grades had larger tumors and a significantly higher prevalence of HCC that was poorly differentiated and had intrahepatic micrometastasis. Other clinicopathological characteristics did not differ significantly among the three groups.

Recurrence-Free Survival and Predictive Factors

Factors associated with recurrence-free survival were evaluated by univariate and multivariate analyses. Univariate analysis showed that age >65 years, HCV infection, HBV infection, elevated DCP level, tumor size >20 mm, presence of multiple tumors, presence of MVI, and presence of intrahepatic metastasis were significant variables affecting recurrence-free survival (Table 2). By multivariate analysis, presence of MVI (mild MVI; hazard ratio [HR]: 1.93, 95 % confidence interval [CI]: 1.25–2.98, $P = 0.003$ and severe MVI; HR: 2.87, 95 % CI: 1.85–4.46, $P < 0.001$), age (>65 years; HR: 1.84, 95 % CI: 1.27–2.65, $P = 0.001$), and number of tumors (2–3; HR: 1.68, 95 % CI: 1.13–2.51, $P = 0.011$) were identified as independent predictors of recurrence-free survival (Table 3). Recurrence-free survival curves of patients stratified by grade of MVI are shown in Fig. 2a. The recurrence-free survival of patients with mild and severe MVI was significantly shorter than that of patients without MVI (no MVI vs. mild MVI, $P = 0.0001$; no MVI vs. severe MVI, $P < 0.0001$; mild MVI vs. severe MVI, $P = 0.1663$).

Pattern and Treatment of First Recurrence after Resection

During the follow-up period, tumor recurrence developed in 122 (54 %) patients, consisting of 48 (47 %) patients without MVI, 38 (64 %) patients with mild MVI, and 36 (80 %) patients with severe MVI. The majority of

TABLE 1 Comparison of patients' characteristics based on grade of microvascular invasion

	No MVI (n = 103)	Mild MVI (n = 59)	Severe MVI (n = 45)	P value
Age, year (range)	65.5 (16–82)	67.0 (34–83)	65.0 (33–81)	0.599
Gender (male/female)	79/24	46/13	37/8	0.754
HCV (positive/negative)	74/29	38/21	35/10	0.319
HBV (positive/negative)	22/81	13/46	11/34	0.917
AST, U/L (range)	43 (15–153)	39.0 (14–137)	41.5 (13–160)	0.838
AFP, ng/ml (range)	11.5 (1–20,764)	10.6 (1.7–5,372)	100.3 (2.8–6,385)†‡	0.001
(≤100/>100)	82/21	45/14	23/22	0.001
DCP, AU/ml (range)	34.5 (10–2,529)	54.5 (10–4,761)	209.5 (13–20,919)†‡	<0.001
(≤100/>100)	77/23	36/23	16/29	<0.001
Tumor size, mm (range)	23.5 (12–50)	26.5 (12–50)†	29 (18–50)†	<0.001
(≤30/>30)	83/20	37/22	25/20	0.002
Number of tumors (single/2–3)	83/20	43/16	34/11	0.505
Histological grade (well/moderate/poorly)	10/92/1	0/52/7	0/33/12	<0.001
Background liver (normal+CH/cirrhosis)	60/43	39/20	27/18	0.61
Intrahepatic micrometastasis (present/absent)	2/101	12/47	23/22	<0.001
Capsular formation (present/absent)	62/41	44/15	25/20	0.09
Type of surgical resection (Major/minor)	57/46	35/24	31/14	0.304

Continuous variables presented as median (range)

MVI microvascular invasion, *HCV* hepatitis C virus, *HBV* hepatitis B virus, *AST* aspartate aminotransferase, *AFP* alpha-fetoprotein, *DCP* des-gamma-carboxy prothrombin, *CH* chronic hepatitis, *well* well differentiated, *moderate* moderately differentiated, *poorly* poorly differentiated

† $P < 0.05$ for post hoc test comparison without MVI

‡ $P < 0.05$ for post hoc test comparison with mild MVI

patients without MVI and with mild MVI who underwent resection for recurrence had intrahepatic recurrence with no more than three tumors (more than 50 % patients had a single tumor) and had no macroscopic VI or extrahepatic metastasis. Consequently, 41 (86 %) patients without MVI and 29 (76 %) patients with mild MVI underwent curative treatment for first recurrence, which included resection, RFA, microwave coagulation therapy (MCT), and percutaneous ethanol injection (PEI). In contrast, patients with severe MVI who underwent resection experienced a high frequency of fatal recurrence, including 22 (61 %) patients with multiple intrahepatic tumors, 6 (17 %) patients with macroscopic VI, and 11 (31 %) patients with extrahepatic metastasis. As a result, curative treatment for first recurrence could only be performed in 15 (42 %) patients with severe MVI.

Disease-Specific Survival and Predictive Factors

Of the total 207 patients, 58 patients died during follow-up. Of these 58 patients, 50 patients died from HCC-related causes. Factors associated with disease-specific survival were evaluated by univariate and multivariate analyses. Univariate analysis showed that presence of cirrhosis, elevated AFP level, elevated DCP level, tumor size >20 mm, presence of multiple tumors, presence of MVI, and presence of intrahepatic metastasis were significant variables affecting disease-specific survival (Table 2). By multivariate analysis, presence of MVI (mild MVI; HR: 2.4, 95 % CI: 1.09–5.26, $P = 0.029$ and severe MVI; HR: 6.06, 95 % CI: 2.93–12.53, $P < 0.001$), background liver (cirrhosis; HR: 2.54, 95 % CI: 1.42–4.55, $P = 0.002$), and tumor size (>30 mm; HR: 3.19, 95 % CI: 1.67–8.71, $P = 0.024$) were identified as independent predictors of disease-specific survival (Table 3). Disease-specific survival curves of patients stratified by grade of MVI are shown in Fig. 2b. Patients with worse MVI grades experienced significantly shorter disease-specific survival (no MVI vs. mild MVI, $P = 0.0017$; no MVI vs. severe MVI, $P < 0.0001$; mild MVI vs. severe MVI, $P = 0.0057$).

DISCUSSION

In our previous study, we demonstrated that MVI was a strong risk factor for poor outcome following curative resection in HCC patients within the Milan criteria.[22] The 3-year, recurrence-free survival rates for patients with and without MVI were 27.7 and 62.5 %, respectively. Thus, the presence of MVI was previously known to lead to a high frequency of recurrence of HCC after liver resection in the

TABLE 2 Univariate analyses of recurrence-free survival and disease-specific survival for hepatocellular carcinoma

	Recurrence-free survival HR (95 % CI)	*P* value	Disease-specific survival HR (95 % CI)	*P* value
Gender				
Male	1.26 (0.79–2)	0.325	1.36 (0.64–2.9)	0.426
Age (year)				
>65	1.71 (1.19–2.46)	0.004	1.03 (0.59–1.79)	0.92
HCV				
Positive	1.73 (1.13–2.65)	0.011	1.16 (0.625–2.16)	0.635
HBV				
Positive	0.58 (0.37–0.93)	0.022	0.95 (0.50–1.83)	0.885
AST, U/L				
>50	1.4 (0.97–2.01)	0.069	1.42 (0.82–2.49)	0.215
AFP, ng/mL				
>100	1.36 (0.93–2)	0.115	1.77 (1–3.12)	0.048
DCP, AU/mL				
>100	1.63 (1.14–2.32)	0.008	1.78 (1.02–3.11)	0.042
Tumor size, mm				
>30	1.64 (1.13–2.38)	0.009	2.66 (1.53–4.64)	0.001
Number of tumors				
2–3	1.93 (1.3–2.87)	0.001	1.92 (1.59–3.5)	0.032
Histological grade				
Moderate	1.56 (0.64–3.84)	0.331	2.78 (0.38–20.19)	0.312
Poorly	1.8 (0.64–5.13)	0.268	3.69 (0.43–31.7)	0.234
Background liver				
Cirrhosis	1.21 (0.84–1.75)	0.3	1.85 (1.06–3.22)	0.03
Microvascular invasion				
Mild	2.16 (1.4–3.31)	<0.001	2.78 (1.29–5.98)	0.009
Severe	2.92 (1.9–4.51)	<0.001	6.61 (3.32–13.16)	<0.001
Intrahepatic micrometastasis				
Present	1.98 (1.27–3.07)	0.002	3.47 (1.91–6.30)	<0.001
Capsular formation				
Present	0.87 (0.6–1.27)	0.482	1.09 (0.61–1.94)	0.771
Type of surgical resection				
Minor	1.18 (0.82–1.69)	0.38	1.64 (0.94–2.86)	0.081

HR hazard ratio, *CI* confidence interval, *HCV* hepatitis C virus, *HBV* hepatitis B virus, *CH* chronic hepatitis, *AST* aspartate aminotransferase, *AFP* alpha-fetoprotein, *DCP* des-gamma-carboxy prothrombin, *well* well differentiated, *moderate* moderately differentiated, *poorly* poorly differentiated

short term.[5–8] Nevertheless, because MVI encompasses many recurrence patterns ranging from curative to fatal, the differences in recurrence patterns are suggested to be associated with a wide range of outcomes with respect to long-term survival. Therefore, we classified patients into two groups (mild and severe MVI) and evaluated the significance of MVI classification.

In the present study, we showed that both mild and severe MVI were significant independent risk factors affecting recurrence-free survival in HCC patients after curative resection. Moreover, our results showed that both patients with mild and severe MVI had a high frequency of micrometastasis in resected liver specimens. Cancer cell spreading via the portal vein has been generally thought to be the main mechanism for such intrahepatic micrometastasis.[25] Micrometastasis is an important cause of early intrahepatic recurrence after liver resection.[26] Consequently, the identification of MVI as a risk factor for early recurrence after curative resection regardless of MVI grade in this study is very relevant.

In addition, both mild and severe MVI were identified as significant independent risk factors affecting survival in HCC patients after curative resection. These results suggest that a high frequency of early recurrence was the primary contributor to poor survival in patients with mild MVI. Early recurrence of HCC is known to be the major risk factor affecting survival following liver resection.[27,28] Moreover, liver function was also identified as an independent risk factor of survival in the present study. Thus, in patients with mild MVI, repeated recurrence and treatment are thought to decrease liver function, thereby contributing

TABLE 3 Multivariate analyses of recurrence-free survival and disease-specific survival for hepatocellular carcinoma

	HR (95 % CI)	*P* value
Recurrence-free survival		
Microvascular invasion		
Mild	1.93 (1.25–2.98)	0.003
Severe	2.87 (1.85–4.46)	<0.001
Age (year)		
>65	1.84 (1.27–2.65)	0.001
Number of tumors		
2–3	1.68 (1.13–2.51)	0.011
Disease-specific survival		
Microvascular invasion		
Mild	2.4 (1.09–5.26)	0.029
Severe	6.06 (2.93–12.53)	<0.001
Background liver		
Cirrhosis	2.54 (1.42–4.55)	0.002
Tumor size (mm)		
>30	2.41 (1.36–4.27)	0.003

HR hazard ratio, *CI* confidence interval

to poor long-term survival.[28] In contrast, although no significant difference in the frequency of recurrence was observed between patients with mild versus severe MVI, patients with severe MVI experienced significantly shorter survival compared with patients with mild MVI. Thus, this observed difference in survival was likely associated with recurrence pattern and not frequency of recurrence. In this study, patients with severe MVI experienced a higher frequency of fatal recurrence, associated with multiple intrahepatic tumors, macroscopic VI, and extrahepatic metastasis. Such fatal recurrence limits additional attempts at curative therapies in HCC patients with severe MVI.[10] As a result, patients with severe MVI experienced poorer survival compared to those with mild MVI. Consequently, we have shown that MVI classification based on the number of invaded vessels can be used to stratify patients into three distinct groups (without MVI, with mild MVI, and with severe MVI) with different risks of survival after curative resection.

Extrahepatic metastasis contributes to poor survival following liver resection in HCC patients.[4,29] Previous studies proposed that MVI was an independent risk factor affecting extrahepatic metastasis in HCC patients after curative resection.[29,30] In agreement with this, the present results revealed that extrahepatic metastasis occurred in approximately 31 % of HCC patients with severe MVI. Liver transplantation is widely accepted as a therapeutic option in HCC patients, particularly for those with cirrhosis and who fulfill the Milan criteria. Recently, MVI has been proposed as a significant risk factor for recurrence and survival in HCC patients after liver transplantation as well as liver resection.[20,21] Because total hepatectomy is performed in the recipient, extrahepatic metastasis is the primary site of recurrence in HCC patients following liver transplantation. Consequently, the present results suggest that severe MVI is a risk factor for liver transplantation in HCC patients, even if they fulfill the Milan criteria.

Prevention of early recurrence of HCC with MVI is the most important strategy for improving long-term survival in HCC patients after curative resection; however, no adjuvant systemic treatment has previously been reported to show a survival benefit. Sorafenib is an oral multikinase inhibitor that has recently become available for advanced HCC. Randomized phase III placebo-controlled trials demonstrated that sorafenib treatment resulted in a significant survival benefit in patients with advanced HCC and maintained liver function; as a result, sorafenib has become the only standard systemic treatment for advanced HCC.[31,32] Consequently, a prospective trial is required to

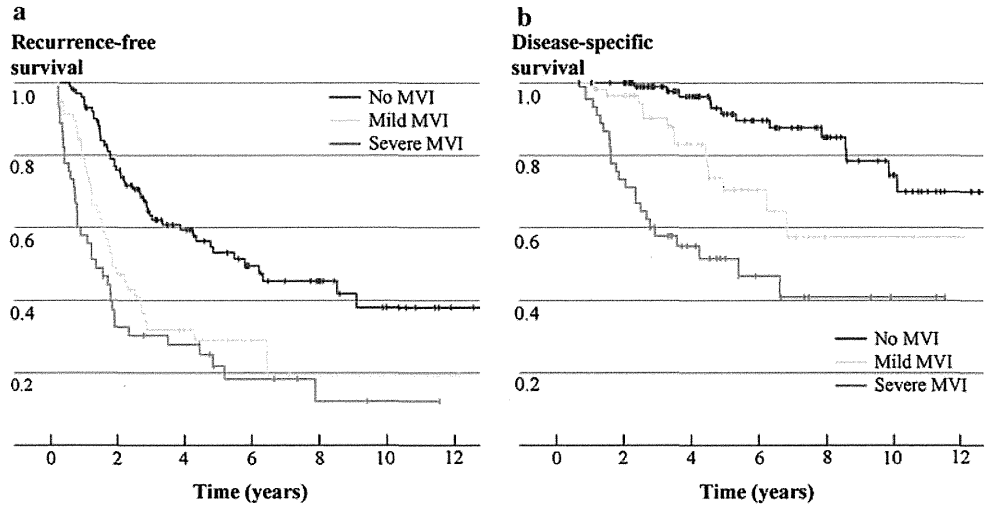

FIG. 2 Recurrence-free survival and disease-specific survival curves of patients stratified by grade of microvascular invasion (MVI). **a** Recurrence-free survival rates at 2 years were 75.9 % in patients without MVI, 47.2 % in patients with mild MVI, and 32.7 % in patients with severe MVI. **b** Disease-specific survival rates at 5 years were 91.5 % in patients without MVI, 70.4 % in patients with mild MVI, and 51.4 % in patients with severe MVI

assess the utility of sorafenib as adjuvant treatment for HCC patients with MVI, particularly because patients with severe MVI experience a high frequency of fatal recurrence after curative resection.

CONCLUSIONS

The present results demonstrated that MVI classification based on number of invaded vessels could stratify different recurrence patterns and risk of survival after curative resection in HCC patients within the Milan criteria. In particular, the presence of severe MVI was found to be associated with high malignant potential of HCC. Therefore, the results of this study suggest that it is important to histologically evaluate the presence of severe MVI after liver resection for determination of strict observation and adjuvant treatment.

DISCLOSURE No commercial interest.

REFERENCES

1. Takayama T, Makuuchi M, Hirohashi S, et al. Early hepatocellular carcinoma as an entity with a high rate of surgical cure. *Hepatology.* 1998;28(5):1241–6.
2. Zhang BH, Yang BH, Tang ZY. Randomized controlled trial of screening for hepatocellular carcinoma. *J Cancer Res Clin Oncol.* 2004;130(7):417–22.
3. Nagasue N, Uchida M, Makino Y, et al. Incidence and factors associated with intrahepatic recurrence following resection of hepatocellular carcinoma. *Gastroenterology.* 1993;105(2):488–94.
4. Yang Y, Nagano H, Ota H, et al. Patterns and clinicopathologic features of extrahepatic recurrence of hepatocellular carcinoma after curative resection. *Surgery.* 2007;141(2):196–202.
5. Okada S, Shimada K, Yamamoto J, et al. Predictive factors for postoperative recurrence of hepatocellular carcinoma. *Gastroenterology.* 1994;106(6):1618–24.
6. Shirabe K, Kanematsu T, Matsumata T, Adachi E, Akazawa K, Sugimachi K. Factors linked to early recurrence of small hepatocellular carcinoma after hepatectomy: univariate and multivariate analyses. *Hepatology.* 1991;14(5):802–5.
7. Portolani N, Coniglio A, Ghidoni S, et al. Early and late recurrence after liver resection for hepatocellular carcinoma: prognostic and therapeutic implications. *Ann Surg.* 2006;243(2):229–35.
8. Imamura H, Matsuyama Y, Tanaka E, et al. Risk factors contributing to early and late phase intrahepatic recurrence of hepatocellular carcinoma after hepatectomy. *J Hepatol.* 2003;38(2):200–7.
9. Park JH, Koh KC, Choi MS, et al. Analysis of risk factors associated with early multinodular recurrences after hepatic resection for hepatocellular carcinoma. *Am J Surg.* 2006;192(1):29–33.
10. Bruix J, Sherman M. Management of hepatocellular carcinoma: an update. *Hepatology.* 2011;53(3):1020–2.
11. Primary liver cancer in Japan. Clinicopathologic features and results of surgical treatment. Liver Cancer Study Group of Japan. *Ann Surg.* 1990;211(3):277–87.
12. Izumi R, Shimizu K, Ii T, et al. Prognostic factors of hepatocellular carcinoma in patients undergoing hepatic resection. *Gastroenterology.* 1994;106(3):720–7.
13. Otto G, Heuschen U, Hofmann WJ, Krumm G, Hinz U, Herfarth C. Survival and recurrence after liver transplantation versus liver resection for hepatocellular carcinoma: a retrospective analysis. *Ann Surg.* 1998;227(3):424–32.
14. Jonas S, Bechstein WO, Steinmuller T, et al. Vascular invasion and histopathologic grading determine outcome after liver transplantation for hepatocellular carcinoma in cirrhosis. *Hepatology.* 2001;33(5):1080–6.
15. Pawlik TM, Esnaola NF, Vauthey JN. Surgical treatment of hepatocellular carcinoma: similar long-term results despite geographic variations. *Liver Transpl.* 2004;10(2 Suppl 1):S74–80.
16. Toyoda H, Kumada T, Kiriyama S, et al. Comparison of the usefulness of three staging systems for hepatocellular carcinoma (CLIP, BCLC, and JIS) in Japan. *Am J Gastroenterol.* 2005;100(8):1764–71.
17. Lang H, Sotiropoulos GC, Brokalaki EI, et al. Survival and recurrence rates after resection for hepatocellular carcinoma in noncirrhotic livers. *J Am Coll Surg.* 2007;205(1):27–36.
18. Roayaie S, Blume IN, Thung SN, et al. A system of classifying microvascular invasion to predict outcome after resection in patients with hepatocellular carcinoma. *Gastroenterology.* 2009;137(3):850–5.
19. Lim KC, Chow PK, Allen JC, et al. Microvascular invasion is a better predictor of tumor recurrence and overall survival following surgical resection for hepatocellular carcinoma compared to the Milan criteria. *Ann Surg.* 2011;254(1):108–13.
20. Bhangui P, Vibert E, Majno P, et al. Intention-to-treat analysis of liver transplantation for hepatocellular carcinoma: living versus deceased donor transplantation. *Hepatology.* 2011;53(5):1570–9.
21. Mazzaferro V, Llovet JM, Miceli R, et al. Predicting survival after liver transplantation in patients with hepatocellular carcinoma beyond the Milan criteria: a retrospective, exploratory analysis. *Lancet Oncol.* 2009;10(1):35–43.
22. Sumie S, Kuromatsu R, Okuda K, et al. Microvascular invasion in patients with hepatocellular carcinoma and its predictable clinicopathological factors. *Ann Surg Oncol.* 2008;15(5):1375–82.
23. Edmondson HA, Steiner PE. Primary carcinoma of the liver: a study of 100 cases among 48,900 necropsies. *Cancer.* 1954;7(3):462–503.
24. Japan LCSGo. General rules for the clinical and pathological study of primary liver cancer. 3rd English edn. 2010.
25. Shi M, Zhang CQ, Zhang YQ, Liang XM, Li JQ. Micrometastases of solitary hepatocellular carcinoma and appropriate resection margin. *World J Surg.* 2004;28(4):376–81.
26. Wang CC, Iyer SG, Low JK, et al. Perioperative factors affecting long-term outcomes of 473 consecutive patients undergoing hepatectomy for hepatocellular carcinoma. *Ann Surg Oncol.* 2009;16(7):1832–42.
27. Shimada K, Sano T, Sakamoto Y, Kosuge T. A long-term follow-up and management study of hepatocellular carcinoma patients surviving for 10 years or longer after curative hepatectomy. *Cancer.* 2005;104(9):1939–47.
28. Poon RT, Fan ST, Lo CM, Liu CL, Wong J. Intrahepatic recurrence after curative resection of hepatocellular carcinoma: long-term results of treatment and prognostic factors. *Ann Surg.* 1999;229(2):216–22.
29. Uchino K, Tateishi R, Shiina S, et al. Hepatocellular carcinoma with extrahepatic metastasis: clinical features and prognostic factors. *Cancer.* 2011;117(19):4475–83.
30. Jun L, Zhenlin Y, Renyan G, et al. Independent factors and predictive score for extrahepatic metastasis of hepatocellular carcinoma following curative hepatectomy. *Oncologist.* 2012;17(7):963–9.

31. Llovet JM, Ricci S, Mazzaferro V, et al. Sorafenib in advanced hepatocellular carcinoma. *N Engl J Med.* 2008;359(4):378–90.
32. Cheng AL, Kang YK, Chen Z, et al. Efficacy and safety of sorafenib in patients in the Asia-Pacific region with advanced hepatocellular carcinoma: a phase III randomised, double-blind, placebo-controlled trial. *Lancet Oncol.* 2009;10(1): 25–34.

Original Research

Comparison Between T1 Relaxation Time of Gd-EOB-DTPA-Enhanced MRI and Liver Stiffness Measurement of Ultrasound Elastography in the Evaluation of Cirrhotic Liver

Masahiro Okada, MD, PhD,[1]* Takamichi Murakami, MD, PhD,[1] Norihisa Yada, MD, PhD,[2] Kazushi Numata, MD, PhD,[3] Minori Onoda, RT,[1] Tomoko Hyodo, MD, PhD,[1] Tatsuo Inoue, MD, PhD,[2] Kazunari Ishii, MD, PhD,[1] and Masatoshi Kudo, MD, PhD[2]

Purpose: To compare four imaging approaches in cirrhotic estimation; pre-enhancement T1 relaxation time (T1RT), reduction rate (RR) of T1RT, signal-based liver-to-muscle ratio (L/M ratio) on gadolinium ethoxybenzyl diethylenetriaminepentaacetic acid (Gd-EOB-DTPA)-enhanced magnetic resonance imaging (MRI), and liver stiffness measurement (LSM) of US elastography.

Materials and Methods: Consecutive 58 patients with chronic liver diseases who underwent both Gd-EOB-DTPA-enhanced MRI and FibroScan were analyzed. Four imaging approaches were evaluated by fibrosis score from liver biopsy and receiver operating characteristic (ROC) analysis.

Results: RR was found to be inversely correlated with LSM ($r=-0.65$). RR decreased with degree of fibrosis (F0-F1, $58.5\pm6.2\%$, versus F2-F3-F4, $48.8\pm11.7\%$, $P=0.010$, F0-F1-F2, $58.2\pm6.2\%$ versus F3-F4, $45.5\pm12.3\%$, $P=0.010$ and F0-F1, $58.5\pm6.2\%$, versus F2-F3, $52.1\pm12.0\%$, $P=0.0038$). LSM increased with degree of fibrosis (F0-F1, 5.4 ± 2.2 kPa versus F2-F3-F3, 19.3 ± 15.5 kPa, $P=0.0011$ and F0-F1-F2, 6.8 ± 3.6 kPa versus F3-F4, 23.8 ± 17.1 kPa, $P=0.0029$ and F0-F1, 5.4 ± 2.2 kPa, versus F2-F3, 11.4 ± 7.2 kPa, $P=0.0098$). Area under ROC curves were 0.83 (F3-F4), 0.72 (F2-F3-F4), 0.68 (F2-F3) for RR and 0.83 (F3-F4), 0.88 (F2-F3-F4), 0.81 (F2-F3) for LSM in discriminating between patients with fibrosis.

Conclusion: The capability by LSM was better than those by RR of T1RT, pre-enhancement T1RT, and L/M ratio to differentiate $F\geq2$, but LSM and RR of T1RT showed the same value to differentiate $F\geq3$.

Key Words: Gd-EOB-DTPA; MRI; US; liver fibrosis; elastography; T1 relaxation time
J. Magn. Reson. Imaging 2013;00:000–000.

HEPATIC FIBROSIS and cirrhosis represent a major public health problem worldwide. Progressive hepatic fibrosis leads to cirrhosis. Liver fibrosis leads to distinct alterations of the hepatic microvasculature, thus increased total hepatic vascular resistance. Early cirrhosis can be reversed by suppression of the fibrotic response (1,2). Common causes of liver cirrhosis are hepatitis C virus (HCV), hepatitis B virus (HBV), alcohol consumption, and nonalcoholic steatohepatitis (NASH). In patients with hepatitis C, progression of hepatic fibrosis is more rapid in those infected at an older age and increases with duration of infection (3).

Routine biochemical and hematological tests fail to quantify liver fibrosis in approximately 50% of patients (4). Liver biopsy is the gold standard in the assessment of liver fibrosis grade. Biopsy involves taking a fraction (~1/50,000th) of the total mass of the liver (5). However, liver biopsy has several limitations including physical discomfort due to its invasive nature. In addition, procedure-related complications such as bleeding (intrahepatic hematoma occurs in up to 6% of patients), bile leak, and pneumothorax can result from liver biopsy, although rare (6).

Ultrasound (US) elastography (7,8) is receiving increasing attention, because there is a need for alternative noninvasive methods to estimate the stage of liver fibrosis. This technology for quantitatively assessing hepatic stiffness has been introduced in the last several years. Liver stiffness measured using US elastography (FibroScan; Echosens, Paris, France) has been validated in the assessment of fibrosis in patients with chronic hepatitis (9). Transient

[1]Department of Radiology, Kinki University Faculty of Medicine, Osaka, Japan.
[2]Department of Gastroenterology and Hepatology, Kinki University Faculty of Medicine, Osaka, Japan.
[3]Gastroenterological Center, Yokohama City University Medical Center, Yokohama, Japan.
*Address reprint requests to: M.O., Kinki University Faculty of Medicine, Department of Radiology, 377-2 Ohno-Higashi, Osaka-Sayama, Osaka 589-8511, Japan. E-mail: mokada@gaia.eonet.ne.jp
Received March 7, 2013; Accepted November 18, 2013.
DOI 10.1002/jmri.24529
View this article online at wileyonlinelibrary.com.